

Sediment characteristics in the North Branch of the Yangtze Estuary based on radioisotope tracers

Zhi-Jun Dai · Jin-Zhou Du · Ao Chu ·
Xiao-Ling Zhang

Received: 20 March 2009 / Accepted: 23 June 2010 / Published online: 1 July 2010
© Springer-Verlag 2010

Abstract Nuclide-specific activity and sediment grain size were analyzed at locations along the North Branch of the Yangtze (Changjiang) Estuary. The spatial distributions of various radioisotopes are presented, along with the sources and applications of these nuclides for studies of the aquatic environment. The specific activities of sediment radionuclides in the North Branch increase toward the ocean, indicating that the sediment is transported from the downstream side of the estuary into the North Branch. The $^{226}\text{Ra}/^{228}\text{Ra}$ ratio agrees well with the observed results and can be used to identify trends in erosion and accretion in the North Branch.

Keywords Radionuclide · Sediment · The Yangtze Estuary · Erosion and accretion

Introduction

Estuaries are complex and special areas with physical, chemical and biological processes that reflect inputs from both land and sea. Unique estuarine biochemical cycles are heavily influenced by absorption, resolution and re-suspension. Isotope tracer technology, especially of natural radioactive isotopes, has been widely applied in Geoscience research (Ivanovich and Harmon 1992) to understand, for

example, chemical evolution and the source and migration of substances. Nuclide radioisotope tracer technology is also important for studying cycles of sediment deposition, biological processes, and the chemistry of the coastal environment (Giffin and Corbett 2003). Previous depositional studies focused mainly on traditional methods, such as grain-size analysis and mineralogy (Gao and Collins 1991, 1992; Giffin and Corbett 2003); few studies have evaluated the distributions and changes of radioisotopes in estuarine sediments. Radioactive isotope studies in estuaries face several challenges: (1) the mechanics of radioisotope absorption and resolution are unclear with limited data; (2) radioactivity is difficult to measure due to the limited activity of nuclides in the depositional environment; and (3) current technology is unable to analyze the long and short half-life times of nuclides such as ^7Be and ^{234}Th .

The aim of this paper is to describe features of the distribution of nuclides in the sediment of the North Branch of the Yangtze Estuary in order to enhance our knowledge of the behavior of nuclides, which can be further applied in the study of morpho-dynamic processes.

Settings and research methods

Setting

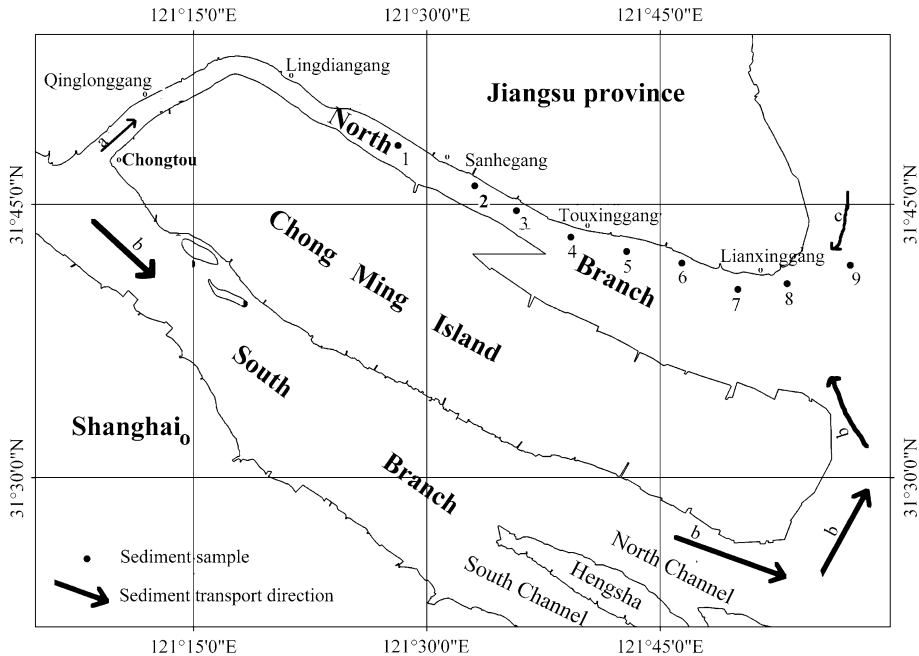
The North Branch is an outlet of the Yangtze Estuary in which sedimentation mainly consists of sand and silt (Yun 2005; Zhou et al. 2005). Semi-diurnal tidal waves propagate in the North Branch and deformation increases inland. Tidal bore occurs at the upper part of the bugle shape. As shown in Fig. 1, the mean tidal ranges at Lianxinggang, Santiaogang and Qinglonggang are 2.93, 3.07, and 2.69 m, respectively (Zhou et al. 2005). The North Branch is

Z.-J. Dai (✉) · J.-Z. Du · X.-L. Zhang
State Key Laboratory of Estuarine and Coastal Research, East
China Normal University, Shanghai 200062, China
e-mail: zjdai@sklec.ecnu.edu.cn

J.-Z. Du
e-mail: jzdu@sklec.ecnu.edu.cn

A. Chu
Hohai University, 1 Xiang Road, Nanjing 210098, China

Fig. 1 Study area and sampling locations



divided into three segments with different topographies and hydrodynamics: the upper reach, the middle reach and the lower reach. Figure 1 also shows that the upper segment from Chongtou to Qinglonggang is controlled by the weakening tide bore. The middle reach from Qinglonggang to Touxinggang is characterized by frequent sedimentation and erosion in the flood channels due to the activity of the tide bore. In the lower reach, from Touxinggang to Lianxinggang, the topography is characterized by shoal-channel patterns due to tidal current (Chen et al. 1982). The hydrodynamics in the North Branch have changed from ebb-dominated in 1958 to flood-dominated today.

Methods

Using a grab sampler, 15-cm-thick sediment samples were collected at locations along the North Branch (Fig. 1) between 21st and 24th of July 2005.

Sediment grain size was analyzed with a laser particle analyzer (LS100Q, Berman, USA). Based on the percentages of each size interval (<0.0005, 0.001, 0.002, 0.004, 0.008, 0.016, 0.032, 0.063, 0.125, 0.25, 0.5 and >1 mm), the mean grain size (μ), sorting coefficient (σ), and skewness (sk) were calculated by the matrix method (Mcmanus 1988). Sediment samples were also classified using Shepard's method (Shepard 1954).

Dried samples were ground and sealed in a plastic box ($\phi 75 \times 70$ mm or $\phi 75 \times 35$ mm) for 3 weeks. The radioactivities of ^{210}Pb , ^{238}U , ^{226}Ra , ^{7}Be , ^{137}Cs , ^{228}Ra , and ^{40}K were measured according to IAEA-recommended procedures (IAEA 1989) with an ADC-1000-I HPGe (Ortec, USA). The relative efficiency was 55%, and the energy

resolution was 1.8 keV (at 1,332 keV). The count time was about 24–36 h. The activities of ^{7}Be , ^{137}Cs , ^{228}Ra , ^{40}K and ^{238}U were determined from the γ -ray peaks at 477.6 keV (10.5%), 661.6 keV (85%), 1,460.8 keV (10.7%) and 63.3 keV (4.24%), respectively. In this study, the overall activity of the total supported and excess ^{210}Pb was evaluated based on its γ -radiation at 46.5 keV (4.25%). The activity of ^{226}Ra was determined at 295.2 keV (19.3%); ^{214}Pb activity was determined at 351.9 keV (37.6%) and 609.3 keV (46.1%), and ^{214}Bi activity was determined at 1,120.3 keV (15%). The activity of ^{228}Ra was calculated as the mean value of its daughter lines, including ^{228}Ac at 338.3 keV (11.27%), 911.2 keV (25.8%) and 969.0 keV (15.8%). The efficiency calibrations of the detector systems were conducted using standard U/Th ore samples (GBW04127). Data reported for the short-lived nuclide ^{7}Be were corrected for the radioactive decay that occurred between sample collection and analysis. Detection limits ranged from 15 Bq kg⁻¹ for ^{40}K to 0.3 Bq kg⁻¹ for ^{137}Cs .

Results

Grain-size characteristics

Sediment grain size is depicted in Fig. 2; the x-axis represents distance from Lingdianggang. Skewness decreases along the North Branch. The mean grain size gradually decreases from 6 ϕ to 8 ϕ toward the ocean, indicating that sediment composition becomes finer along the North Branch. In addition, sediment sorting is poor and has a sorting coefficient of around two.

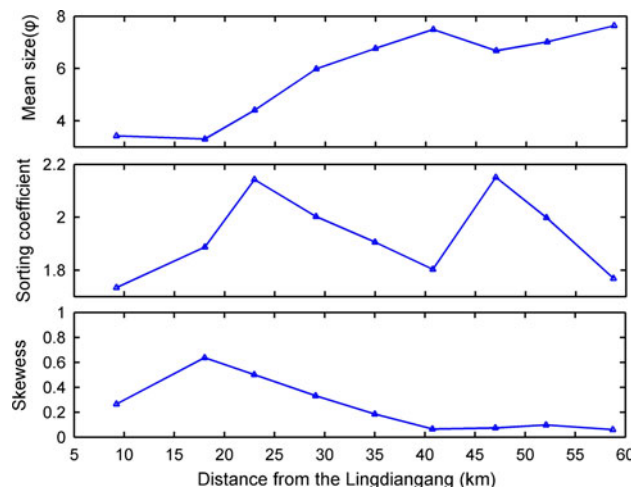


Fig. 2 Sediment grain-size characteristics along the North Branch

Characteristics of nuclides in sediment

Most studies on coastal and near-shore nuclides have used sediment cores for chronology, and very few have considered the characteristics of nuclides in estuarine sediment. This study measured the specific activities of ^{210}Pb , ^{234}Th , ^{226}Ra , ^7Be , ^{228}Ra , ^{137}Cs and ^{40}K , which are listed in Table 1. The specific activity of ^{210}Pb varies from 21.7 ± 3.7 to 47.0 ± 4.3 Bq/kg, which is lower than that of the South China Sea (48 Bq/kg; Liu et al. 2001a, b). The specific activity of ^{238}U varies from 24.7 ± 4.3 to 40.7 ± 4.5 Bq/kg. The specific activity varies between 29.4 ± 1.5 and 52.5 ± 2.2 Bq/kg for ^{228}Ra , from 425 ± 8 to 704 ± 12 Bq/kg for ^{40}K , and between 0.45 ± 0.17 and 2.27 ± 0.36 Bq/kg for ^{137}Cs . The specific activity of ^7Be is below the detection limit.

The results in Table 1 are summarized in Fig. 3, which shows the distributions of the specific activities of each nuclide along the North Branch. Because specific activity is positively correlated with distance from Lindiangang, the

specific activities of each sediment nuclide increase toward the ocean.

Discussion

Sediment transport

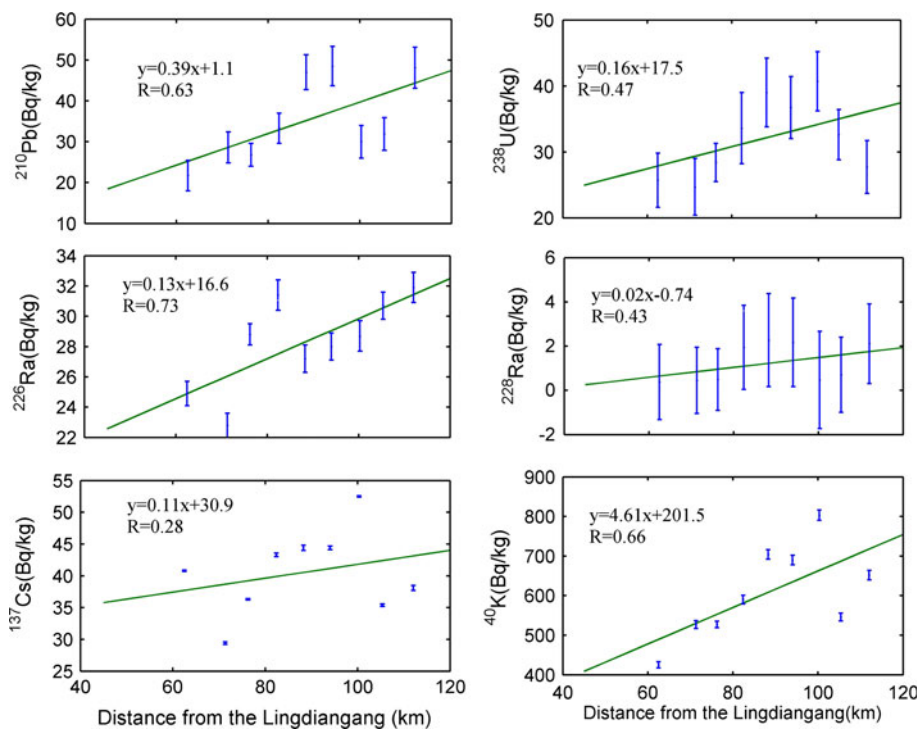
In general, the specific activity of a nuclide in the sediment is controlled by its source and is affected by the processes of absorption, resolution and re-suspension. The source of ^{226}Ra is uranium mining, and it is transported from land to sea (Liu et al., 2001a, b). The activities of ^{210}Pb and ^{226}Ra decrease as these nuclides are transported from land to sea. The artificial nuclide ^{137}Cs is generated from nuclear testing and is found in rivers and air. The specific activity of ^{137}Cs typically decreases seaward (Liu et al., 2001b). In sum, previous studies found that specific activities of sediment nuclides decrease toward the ocean.

In contrast, however, the specific activities of nuclides in the North Branch of the Yangtze Estuary increase toward the ocean. Several explanations of this phenomenon are possible. First, before the 1950s, the North Branch was ebb-dominated and carried materials from upstream, as shown by arrow a in Fig. 1 (Chen et al. 1982). Since 1958, the North Branch has been flood-dominated and has received a greater proportion of materials from the ocean. This reversed net flux in the sector between Chongtou and Lianxinggang has been observed since 2001 (Chen et al. 2003). Thus, the observed pattern of nuclide-specific activities may indicate the influence of sediment from the direction of the ocean rather than from inland. As a second possibility, the pattern of nuclide-specific activities may be controlled by complex physical processes in the Yangtze Estuary. Because previous research has suggested that the specific activities of nuclides in the Yangtze Estuary are much higher than those in the offshore zone (Liu et al. 2001b), sediments in the North Branch with high nuclide-

Table 1 Specific activity of radioisotope in sediment along the North Branch

Sample indexes	Measured results (Bq/kg)						
	^{210}Pb	^{238}U	^{226}Ra	^7Be	^{228}Ra	^{137}Cs	^{40}K
1	21.7 ± 3.7	25.7 ± 4.1	24.9 ± 0.8	<2.7	40.8 ± 1.7	0.37 ± 0.1	425 ± 8
2	28.6 ± 3.8	24.7 ± 4.3	22.8 ± 0.8	<2.9	29.4 ± 1.5	0.45 ± 0.2	527 ± 10
3	26.8 ± 2.8	28.4 ± 2.9	28.8 ± 0.7	<2.4	36.3 ± 1.4	0.49 ± 0.1	527 ± 8
4	33.3 ± 3.7	33.6 ± 5.4	31.4 ± 1.0	<3.2	43.3 ± 1.9	1.94 ± 0.3	590 ± 11
5	47.0 ± 4.3	39.0 ± 5.2	27.2 ± 0.9	<3.5	44.4 ± 2.1	2.27 ± 0.4	704 ± 12
6	48.5 ± 4.8	36.7 ± 4.7	28.0 ± 0.9	<3.5	44.4 ± 2.0	2.17 ± 0.3	690 ± 12
7	30.0 ± 4.0	40.7 ± 4.5	28.7 ± 1.0	<3.6	52.5 ± 2.2	0.47 ± 0.1	803 ± 13
8	31.9 ± 4.0	32.6 ± 3.8	30.7 ± 0.9	<3.2	35.4 ± 1.7	0.71 ± 0.2	546 ± 10
9	48.1 ± 5.0	27.7 ± 4.0	31.9 ± 1.0	<3.4	38.1 ± 1.8	2.11 ± 0.4	652 ± 12

Fig. 3 Distribution of the specific activities of nuclides along the North Branch



specific activities must not originate on the continent shelf of the East China Sea. Therefore, the source of sediment in the North Branch can only be the Yangtze River, as indicated by arrow b in Fig. 1. Finally, previous studies have confirmed that a large amount of sediment from the South Branch of the Yangtze Estuary is transported into the North Branch (Yun 2005). Minor sediment from the Jiangsu Coast may also be transported into the North Branch, as indicated by arrow c in Fig. 1 (Yun 2005; Zhou et al. 2005). Thus, sediment in the North Branch is mainly transported from the South Branch along arrow b, which causes the specific activities of the nuclides to decrease inland along the North Branch.

This study also evaluated ^{7}Be , which is produced by the interaction of cosmic rays with N and O in air and can then be transported downstream along with water and suspended sediment. Although ^{7}Be can move into sediment quickly, its activity in North Branch sediments is below detection limits.

Based on statistical analysis, it appears to be difficult to trace sediment processes using an individual nuclide (Fig. 3). This may be due to the “particle effect” for a single nuclide on a particle. Nevertheless, the “pair” of Ra isotopes (^{226}Ra and ^{228}Ra) may form a good tracer.

Evaluation of accretion and erosion using $^{226}\text{Ra}/^{228}\text{Ra}$

Previous studies have also suggested that ^{226}Ra and ^{228}Ra could be important tracers of sediment transport processes (Stantschi 1983). The mobility of ^{228}Ra is higher than that

of ^{226}Ra (Bai and Wan 1998). Although both are present in the crystal framework of clay minerals, the carbonate and exchangeable phases contain distinctly more ^{228}Ra than ^{226}Ra . As a result, ^{228}Ra in sediment can be more easily eroded and transported than ^{226}Ra . In order to reduce the effects of sediment grain size and composition on analytical results, the ratio between ^{226}Ra and ^{228}Ra is used to describe erosion and accretion. A $^{226}\text{Ra}/^{228}\text{Ra}$ ratio larger than one suggests erosion, and vice versa (Bai et al. 1997).

Therefore, the ratio of $^{226}\text{Ra}/^{228}\text{Ra}$ is applicable for assessing erosion and accretion in the North Branch. Values of $^{226}\text{Ra}/^{228}\text{Ra}$ and accretion for each location are shown in Table 2. All $^{226}\text{Ra}/^{228}\text{Ra}$ ratios are less than one, which is consistent with the expected accretion along the North Branch. Although no recent data for the water depth difference is available, data collected between 1978 and 1997 are reasonably representative of the erosion/accretion trend because hydrodynamic conditions along the North Branch have remained consistent. On this basis, Table 2

Table 2 $^{226}\text{Ra}/^{228}\text{Ra}$ and erosion/accretion at each location

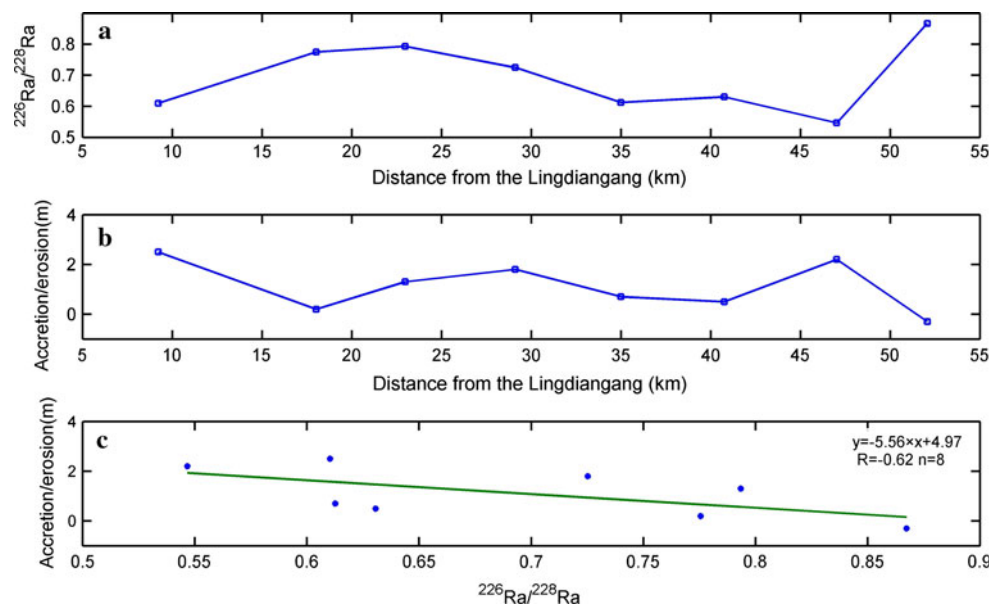
Location	1	2	3	4	5	6	7	8	9
$^{226}\text{Ra}/^{228}\text{Ra}$	0.61	0.78	0.79	0.73	0.61	0.63	0.54	0.87	0.84
Accretion (m) ^a	2.5	0.2	1.3	1.8	0.7	0.5	2.2	-0.3 ^b	-

^a According to water depth difference between in 1978 and in 1997 at each location

^b Minus means erosion

- No data available

Fig. 4 Correlation of $^{226}\text{Ra}/^{228}\text{Ra}$ with erosion and accretion along the North Branch



shows that accretion did occur between 1978 and 1997 at all locations except location 8. Location 8 is at the entrance of the North Branch and is therefore exposed to strong currents and waves, which cause large errors in depth measurement. Table 2 was used to obtain Fig. 4. Figure 4a shows $^{226}\text{Ra}/^{228}\text{Ra}$ ratios at locations along the North Branch. Relatively small values around locations 1 and 7 indicate greater accretion. Figure 4b shows historical accretion at all locations in the North Branch. Intense accretion is observed at locations 1 and 7, in agreement with the $^{226}\text{Ra}/^{228}\text{Ra}$ distribution mentioned above. The apparent relationship between $^{226}\text{Ra}/^{228}\text{Ra}$ and accretion in the North Branch is shown in Fig. 4c. The relationship is good and has 90% significance. According to this relationship, smaller $^{226}\text{Ra}/^{228}\text{Ra}$ ratios are associated with higher accretion. This phenomenon is caused by the previously mentioned isotope “pair.” When the “pair” of nuclides enter into the estuary on riverine particles and desorb, their properties are similar in seawater. As mentioned above, $^{226}\text{Ra}/^{228}\text{Ra}$ ratios greater than 1 suggest that erosion is occurring and vice versa (Bai et al. 1997). For the same reason, riverine particles are more likely to release ^{228}Ra than ^{226}Ra to water in the estuary. After a long time desorption with seawater leach, the activity of ^{228}Ra in sediment in seaward is much lower than the activity of ^{226}Ra . It means that more “fresh” the sediment, shorter the time for ^{228}Ra to be desorbed from particle and higher the activity of ^{228}Ra in comparison with that of ^{226}Ra . Therefore, the greater deposition (accretion) of riverine particles (more “fresh”) means much higher ^{228}Ra activity than that of ^{226}Ra in surface sediment, and yields a lower ratio of $^{226}\text{Ra}/^{228}\text{Ra}$, vice versa.

Thus, the ratio of $^{226}\text{Ra}/^{228}\text{Ra}$ in sediments can be used to investigate erosion and accretion in estuaries.

Conclusions

This analysis of the specific activities of nuclides in sediment reveals that sediment in the North Branch originates from the Yangtze River, which has a much higher nuclide-specific activity. As indicated by the fact that the specific activities of nuclides increase toward the ocean, most sediment enters the North Branch from its mouth rather than from upstream. This pattern is consistent with the shift from an ebb-dominated system in 1958 to the current flood-dominated regime. Values of $^{226}\text{Ra}/^{228}\text{Ra}$ are smaller than 1, consistent with the expected accretion in the North Branch. Measurements of accretion agree well with expected $^{226}\text{Ra}/^{228}\text{Ra}$ ratios. Thereafter, nuclide-specific activities can identify sediment origin, and $^{226}\text{Ra}/^{228}\text{Ra}$ ratios may be a valuable new tool for predicting erosion and accretion in estuaries.

Acknowledgments This research was supported by the National Science Key Foundation in China (50939003) and the National Science Foundation in China (Grant Nos. 40976054; 40976055). We thank two anonymous reviewers for valuable comments that helped to improve the manuscript.

References

- Bai ZG, Wan GJ (1998) Progress in the study of the soil erosion using radionuclides. *Adv Earth Sci* 13(1):232–237 (in Chinese with English abstract)
- Bai ZG, Wan GJ, Wang CS (1997) Geochemical speciation of soil ^{7}Be , ^{137}Cs , ^{226}Ra , ^{228}Ra as tracers to particle transport. *Pedosphere* 7(3):263–268
- Chen JY, Yun CX, Xu HG (1982) The model of development of the Yangtze Estuary during the last 2000 years. In: Kennedy VSZ (ed) *Estuarine comparisons*. Academic Press, New York, pp 655–666

- Chen SL, Chen JY, Gu GC (2003) The tidal bore on the north branch of Yangtze Estuary and its effects on the estuary. *J East China Normal Univ (Nat Sci)* 2:74–80 (in Chinese with English abstract)
- Gao S, Collins M (1991) A critique of the “McLaren Method” for defining sediment transport paths. *J Sediment Petrol* 61:143–146
- Gao S, Collins M (1992) Net sediment transport patterns inferred from grain-size trends, based upon definition of “transport vectors”. *Sediment Geol* 80:47–60
- Giffin D, Corbett DR (2003) Evaluation of sediment dynamics in coastal systems via short-lived radioisotopes. *J Mar Syst* 42:83–96
- IAEA (1989) Measurement of radionuclides in food and the environment: a guidebook. Technical Reports Series. No. 295. IAEA, Vienna
- Ivanovich M, Harmon RS (1992) Uranium series disequilibrium: applications to environmental problems. Clarendon Press, Oxford
- Liu GS, Huang YP, Chen M, Qiu YS (2001a) Distribution features of radionuclides in surface sediments of Nansha Sea areas. *Mar Sci* 25(8):1–5 (in Chinese with English abstract)
- Liu GS, Huang YP, Chen M, Qiu YS (2001b) Specific activity and distribution of natural radionuclides and ^{137}Cs in surface sediments of the northeastern South China Sea. *Acta Oceanol Sin* 23(6):76–84 (in Chinese with English abstract)
- Mcmanus J (1988) Grain size determination and interpretation. In: Tucker M (ed) *Techniques in sedimentology*. Blackwell, Oxford, pp 63–85
- Shepard FP (1954) Nomenclature based on sand–silt–clay ratios. *J Sediment Petrol* 24:151–158
- Stantschi PH (1983) Radioisotopes in aquatic sciences. AWAG/News 14/15:1–6
- Yun CX (2005) The law of basic evolution in Changjiang Estuary. China Ocean Press, Beijing, vol 2, pp 81–89 (in Chinese with English abstract)
- Zhou KS, Meng Y, Liu CZ, Hong XQ (2005) Characteristics of aggradation and granularity for the north branch of Changjiang River estuary and its environmental implication. *Mar Geol Lett* 21(11):1–7 (in Chinese with English abstract)